Solid-state thin-films lithium batteries for integration in microsystems

J. F. Ribeiro[1], M. F. Silva[1], J. P. Carmo[1], L. M. Gonçalves[1],
M. M. Silva[2] and J. H. Correia[1]

[1]University of Minho, Algoritmi Center, Azurem, Guimaraes, PORTUGAL

[2]University of Minho, Chemistry Center, Gualtar, Braga, PORTUGAL

[1]{jribeiro, fsilva, jcarmo, lgoncalves, higino.correia}@dei.uminho.pt

[2]nini@quimica.uminho.pt

ABSTRACT

The increasing miniaturization of electronic devices requires the miniaturization of devices that provide energy to them. Autonomous devices of reduced consumption are increasingly common and they have benefited from energy harvesting techniques. However, these devices often have peak power consumption, requiring the storage of energy.

This chapter presents the fabrication and characterization of thin-films for solid-state lithium battery. The solid-state batteries stand out for the possibility of all materials being solid and therefore ideal for microelectronics fabrication techniques. Lithium batteries are composed primarily of three materials, the cathode, the electrolyte and the anode. The positive electrode (cathode) and negative (anode) have high electrical conductivity and capacity of extraction and insertion of lithium ions. The electrolyte's main features are the high ionic conductivity and high electrical resistivity. The materials chosen for the battery are lithium cobalt oxide (cathode), lithium phosphorus oxynitride (electrolyte) and lithium metal (anode).

The lithium cobalt oxide cathode ($LiCoO_2$) was deposited by RF sputtering and characterized using the techniques XRD, EDX, SEM and electrical resistivity. Fully crystalline $LiCoO_2$ was achieved with an annealing of 650 °C in vacuum for two hours. Electrical resistivity of 3.7 Ωmm was achieved.

The lithium phosphorus oxynitride electrolyte (LIPON) was deposited by RF sputtering and characterized using the techniques EDX, SEM, ionic conductivity, DSC and TGA. Ionic conductivity of $6.3\text{x}10^{-7}$ Scm^{-1} for a temperature of 26 °C was measured. It was also proven the thermal stability of LIPON up to 400 °C.

The metallic lithium anode (Li) was deposited by thermal evaporation and its electrical resistance measured at four points during the deposition. Resistance of about 3.5 Ω was measured for a thickness of 3 µm. The oxidation rate of the lithium in contact with the ambient atmosphere was evaluated. The patterning process of the battery was developed by means of shadow masks.

Keywords: Battery, lithium and thin-film.

1 INTRODUCTION

1.1 THIN-FILMS BATTERIES

A battery is an energy source that converts chemical energy into electrical energy [1].Each battery consists of an electrolyte and two electrodes. The electrolyte is essentially an excellent ionic conductor and an excellent electrical insulator. The electrodes are designated as cathode (positive electrode) and anode (negative electrode) and are essentially good electrical conductors, capable of insertion and extraction of ions. The battery produces electric current when an atom or molecule becomes an ion by electron transfer [2]. The electron is released into an external circuit via an oxidation reaction. The ion resulting from the oxidation reaction will flow through the electrolyte and a counter reaction, the reduction will occur at the cathode. The electron transfer reactions, known as redox reactions, occur among a set of chemical species. In battery case, the anode is the reducer and the cathode is the oxidant, in other words, the anode gives electrons and the cathode has the capacity to receive them. The change between the type of charge carriers between the electrolyte and the electrode forces the reaction between the connection electrode/electrolyte [3]. Fig. 1 shows a simplified schematic of a battery.

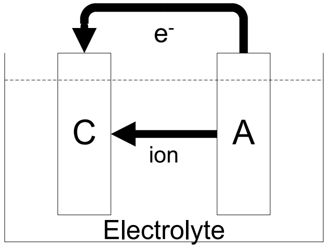

FIG. 1: SIMPLIFIED SCHEMATIC OF BATTERY DISCHARGE, WHER C IS THE CATHODE AND A IS THE ANODE.

Provide power to an external circuit through redox reactions is called battery discharge. The redox reaction is possible only when a battery cathode and anode have a different chemical potential [2]. The chemical potential is equivalent to the electric potential in an electronic circuit by analogy. The chemical potential of a material is the partial molar free energy of Gibbs of this element in a solution [4]. Thus we can consider it the driving force for the diffusion of atoms in a broad sense of the word. The battery is rechargeable when the cathode and anode also have the capacity to release and receive electrons respectively. Recharging the battery takes place by applying a reverse voltage and higher than the operating voltage of the battery, thereby forcing the electrons and ions to flow back to the battery anode. This process is called battery charge.

1.2 BATTERY EVOLUTION

The electric battery was invented by Alessandro Volta (Fig. 2) in late 1799 [5], who announced his invention to the Royal Society of London in 1800. The investigation led to the development of this device began in 1792, after Volta read the work of Luigi Galvani [6]. The work of Galvani reported the existence of intrinsic electricity in living organisms [7].

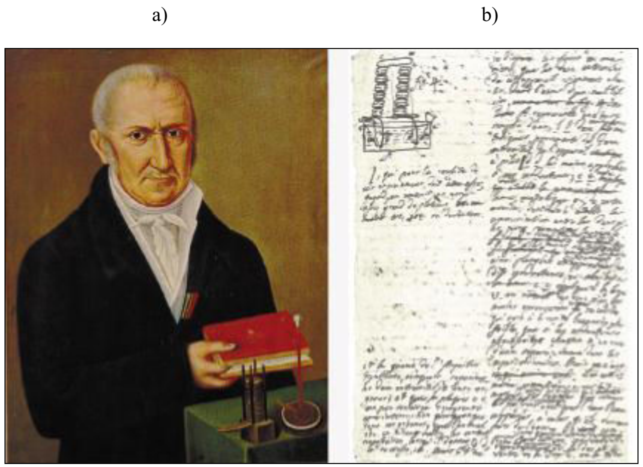
a) b)

FIG. 2: ALESSANDRO VOLTA: A) CONTEMPORARY PICTURE, B) LETTER OF PAGE THAT ANNOUNCE THE ELECTRIC BATTERY [8].

In 1802, Dr. William Cruickshank designed the first electric battery capable of being mass-produced. Cruickshank had managed to obtain copper sheets into squares, which were welded to the edge of sheet zinc with the same size. These sheets were placed inside a rectangular wooden box, which was then sealed with cement. After putting the plates in position, the box was filled with an electrolyte of brine solution (water saturated with salt). John F. Daniell, an English chemist, developed in 1836, a battery with a better and more stable current than the device of Volta. He tries to find a solution to the problem of hydrogen bubbles found in the Volta battery, adding a second electrolyte to consume hydrogen [6]. In 1844, William Robert Grove developed a battery with a higher current than that of Daniell and nearly twice the voltage. This consisted of a platinum cathode immersed in nitric acid and a zinc anode immersed in sulphuric acid, separated by porous clay.

Gaston Planté, French physicist, has invented the first rechargeable battery in 1859. This battery was based on lead-acid chemistry that is still used [9]. During the 1860s came a variant of the Daniell battery, invented by Callaud, which dispensed the porous barrier that allow the increase of current. In 1866, Georges Leclanché invented a battery with a manganese dioxide cathode, a zinc anode and an electrolyte of ammonium chloride, known as a battery of Leclanché. Several scientists have tried to find a battery consists of only solid materials to be easier to use. Carl Gassner in 1886 obtained a German patent of a variant of Leclanché battery, which came to be known as the dry battery, because the electrolyte was not a free liquid [6].

In 1899, Waldmar Jungner from Sweden invented the nickel cadmium battery, with the positive electrode of nickel, the negative electrode of cadmium and an electrolyte solution of potassium hydroxide [9]. Two years later, Edison replaced cadmium by iron formed nickel-iron battery. At this point, the nickel-cadmium and nickel-iron was expensive due to the cost of their materials and therefore their limited applications. The nickel cadmium batteries became available only after, in 1932, Shlecht and Ackermann improve the load current and longevity of batteries, and after Neumann can completely seal the batteries in 1947 [6].

Lewis Urry, an engineer who worked for Energizer, was tasked to improve the longevity of zinc-carbon battery. Urry decided that this was not the best solution and dedicated to the development of alkaline batteries with a manganese dioxide cathode, an anode of zinc powder and an alkaline electrolyte [10]. This battery became commercially available in 1959. The batteries of nickel metal hydride appeared on the market in 1989 as a variation of the nickel-hydrogen batteries, which arisen in 1970.

The early research on lithium secondary batteries back to the years of 1960 – 1970 due to the energy crisis and the growing interest in energy sources for mobile applications [6]. However, no breakthrough was achieved before 1991 and there is still a major deficiency in power and energy density of secondary batteries. John B. Goodenough, in 1980, led a team of Sony in the investigation of Li-ion batteries. These batteries came on the market in 1991 [11, 12].The lithium polymer batteries were launched in 1996, introduced greater flexibility and energy density [13]. Lithium solid state batteries only emerged in 2009, released by the company Cymbet [14]. The Table 1 summarizes the history of batteries.

TABLE 1: BATTERY HISTORY [6].

Battery history		
1600	Gilbert (English)	Established the electrochemical study
1791	Galvani (Italian)	Discovered the ‘animal electricity’
1800	Volta (Italian)	Electrical battery inventor
1802	Cruickshank (English)	First electrical battery capable of mass-production
1820	Ampère (France)	Electricity through magnetism
1833	Faraday (English)	Faraday’s law announcement
1836	Daniell (English)	Daniell’s battery invention
1844	Grove (Wales)	Grove’s battery invention
1859	Planté (France)	Lead-acid battery invention
1868	Leclanché (France)	Leclanché’s battery invention
1888	Gassner (USA)	Dry battery completion
1899	Jungner (Sweden)	Nickel-cadmium battery invention
1901	Edison (USA)	Nickel-iron battery invention
1932	Shlecht and Ackermann (Germany)	Cluster plate invention
1947	Neumann (France)	Nickel-cadmium battery successfully sealed
1960	Union Carbide (USA)	First alkaline battery development
1970		Development of valve regulated for lead-acid batteries
1990		Sales of hydride nickel-metal batteries
1992	Kordesch (Canada)	Marketing of rechargeable alkaline batteries
1999		Marketing of polymer lithium ion batteries
2009	Cymbet (USA)	Marketing of solid-state lithium ion batteries

Currently most attempts to improve the batteries face the problem of macro scale, but work is now being directed to the nano scale [15]. The nano materials were slow to enter in the energy storage market because the effective increase in surface area of the electrodes increases the risk of adverse reactions involving the decomposition of the electrolyte. Only in 2000 was perceived that such reactions can be controlled by coating the electrodes to protect them from oxidation and reduction reactions unwanted. The work on nano materials gave new life to lithium-ion batteries [16]. Nano materials allow benefits in terms of capacity, power, energy density and cost of lithium ion batteries and are still far from being fully exploited [15], making it increasingly important for energy storage [17-19]. In the coming decades the batteries may also evolve into the use of organic materials. Today is already under investigation the feasibility of using $Li_XC_6O_6$ active molecules, which can be prepared from natural sugars [20].

In Table 2 presents a comparison between lithium and other battery types. The first column indicates the type of battery; the second indicates the voltage produced and the third the gravimetric energy density (Wh/kg) and volumetric energy density (Wh/l) reached with the respective type of battery. The fourth and fifth column show the maximum discharge time at constant current for the battery depending on thickness.

TABLE 2: COMPARISON OF LITHIUM BATTERIES WITH OTHER TYPE OF BATTERIES [21].

Battery type	Voltage (V)	Energy density (Wh/kg–Wh/l)	Discharge time for 5 mm thickness (hh:mm:ss)	Discharge time for 1 mm thickness (hh:mm:ss)
Ni-Cd	1,2	40-100	11:15:00	00:05:24
Ni-MH	1,2	90-245	27:36:00	00:13:12
Ag-Zn	1,5	110-220	24:45:00	00:11:54
Li-ion	3,6	155-400	45:00:00	00:21:36
Li-polymer	3,6	180-380	42:45:00	00:20:24
Thin-film Li-ion	3,6	250-1000	112:30:00	00:54:00

1.3 MOTIVATION FOR THIN-FILMS BATTERIES

One of the great challenges of the 21st century is undoubtedly the production and storage of energy. The increased reduction in energy consumption by electronic devices, either in current or voltage supply, has allowed the creation of autonomous wireless devices without needed external power supply. The wireless autonomous devices have also benefited from the improvement of energy harvesting techniques, which allow the use of various types of energy from the environment (heat, light, vibration, etc.). However these devices require a battery capable of powering the circuit when the power source is not available and permits the levelling of energy consumption, since the wireless devices have peak consumption when they are transmitting information and very low power consumption in the remaining period of time.

The need for remote electronic devices is increasing and batteries increasingly play a key role in viability and minimum size of these same devices. Thus, the integration of the battery in the microchip increases the electronic circuit integration and miniaturization of devices, enabling further cost reduction. Lithium batteries have been highlighted by the possibility of all materials be solid such they are ideal to fabricate using thin-film techniques, allowing their integration in integrated circuits. The solid-state batteries (all constituent materials are solid) are intrinsically safe, can withstand temperatures of welding and present faster time of charge/discharge than conventional batteries. These batteries can also be manufactured in any shape and size without increasing costs in miniaturization of the same. The Fig. 3 illustrates a possible design for solid-state lithium batteries, using lithium cobalt oxide ($LiCoO_2$) as cathode, the lithium phosphorus oxynitride (LIPON) as electrolyte and metallic lithium as anode.

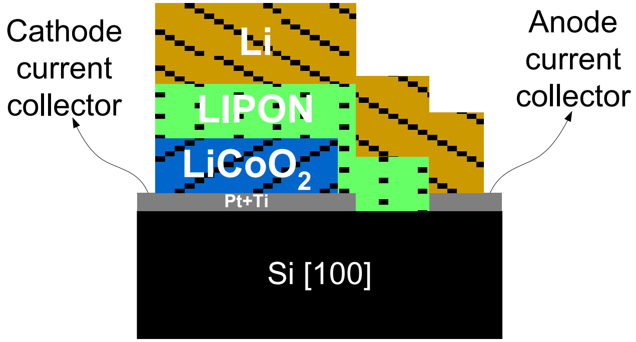

FIG. 3: DESIGN OF A THIN-FILM BATTERY.

1.4 APPLICATIONS

Thin-film batteries have a high range of applications, like energy harvesting modules, wireless sensors and medical devices. This kind of batteries is especially profitable for remote and autonomous devices. Nowadays must of remote devices are size and life limited by their battery. Conventional batteries are huge in comparison with the must electronic devices and have a very long time of charge difficulty the applications of energy harvesting power sources. Thin-film batteries can be charge/discharge in less than a minute.

2 LITHIUM BATTERIES

2.1 SOLID-STATE BATTERIES

In conventional batteries the electrolyte is usually an acid or an alkaline solution containing dissolved metal ions or an organic solvent consisting of salts with metal ions [2]. Liquid electrolytes have advantages as a high ionic conductivity, high electrical resistivity and an excellent contact with the electrodes. Despite the advantages liquid electrolytes have serious disadvantages such as corrosion of the electrodes. Batteries with liquid electrolytes also require an airtight package to ensure its security and stability. This type of encapsulation adds weight and reduces the energy density of a battery.

A solid state electrolyte, in addition to ensuring a high ionic conductivity and high electrical resistance, must ensure good contact and good chemical stability with the electrodes [2]. An excellent energy density can be achieved with solid-state batteries, due to reduced size and encapsulation of the battery [21].

2.2 STATE OF THE ART

The thin-film batteries emerged in 1982 [21], when the Japanese company Hitachi announced a thin-film solid state battery. The advertised battery comprises a cathode of TiS_2 deposited by chemical vapour deposition (CVD), an electrolyte of $Li_{3,6}Si_{0,6}P_{0,4}O_4$ deposited by RF sputtering and an anode of lithium metal deposited by thermal evaporation. It was also tested $WO_3V_2O_5$ as cathode deposited by sputtering in a H_2-Ar plasma [22].

A second approach was the replacement of the liquid electrolyte by a polymer electrolyte. This technology was restricted to large systems (traction power or backup power) because only withstand temperatures up to 80 °C [23]. Shortly after, several research groups have attempted to develop a hybrid electrolyte, in the hope of combining the advantages of the polymer electrolyte without the risks associated with use of lithium metal. A hybrid electrolyte comprises a polymer matrix with a liquid solvent and a salt. Companies such as Valence and Danionics were involved in the development of polymer batteries, but they never were commercialized on a large scale because safety issues [21].

In 1991, Sony sold a lithium-ion battery with a $LiCoO_2$ cathode and a carbon anode [11, 12]. This type of lithium-ion batteries had a potential exceeding 3.6 V (three times longer than alkaline batteries) and gravimetric energy densities of 120-150 WhKg^{-1} (two to three times higher than the nickel-cadmium). These batteries have become ideal for portable electronic devices.

The company NTT Group of Japan has also developed thin-film batteries that used $Li_{3,4}V_{0,6}Si_{0,4}O_4$ as electrolyte and $LiCoO_2$ [24] or $LiMn_2O_4$ [25] as cathode, deposited by RF sputtering. The battery has 1 cm^2 with cathode thickness of 1 to 5 µm, electrolyte thickness of 1 µm and lithium anode thickness of 4 to 8 µm. Thin-film batteries were also developed by Bellcore and Battery companies in 1980. They used an electrolyte of $Li_4P_2S_7$ or Li_3PO_4-P_2S_5, a cathode of TiS_2 and an anode of lithium or LiI. The Bellcore also announced a lithium battery with $LiMn_2O_4$ cathode, an electrolyte of LiBP or lithium phosphorus oxynitride (LIPON) and a lithium metal anode. The displayed battery operated between 3.5 and 4.3 V and had a capacity of 70 µA/cm^2 to more than 150 cycles [26]. A group at Oak Ridge National Laboratory (ORNL), USA, devoted himself to research of thin-film batteries using an electrolyte of LIPON. The LIPON is deposited by RF sputtering with a target of Li_3PO_4 in a nitrogen atmosphere, and shows high stability compared with lithium oxides or sulphates. Despite LIPON be more stable, it has a moderate ionic conductivity of 2.3 x10^{-6} Scm^{-1} at room temperature and activation energy of 0.55 eV [27]. The potential curve indicates a range of stability of LIPON from 0 to 5.5 V against a lithium electrode. The battery anode (lithium metal) was deposited by thermal evaporation and cathode ($LiCoO_2$ or $LiMn_2O_4$) and electrolyte (LIPON) was deposited by RF sputtering. The ORNL group also investigated some combinations of electrodes with the electrolyte LIPON, and got a very good performance for voltages between 2 and 5 V, a current density to 10 mA/cm^2, and more than 10,000 cycles of charge/discharge [28]. Neudecker, *et al.*, a researcher from ORNL, reported a Li-free thin film battery, where the lithium anode and the anode current collector are replaced by a single layer of copper [29]. This battery is quite useful when you want to use a method of welder, since lithium has a melting temperature of 178 °C [29], below the temperature used for soldering processes. The LIPON is now recognized as a standard solid electrolyte for thin-film batteries and has been used by many groups, especially in private companies at USA [1]. The LIPON is also used by Park *et al.* [30], Korea and Baba *et al.* [31], Iwate University in Japan. Baba, *et al.*, reported thin-film batteries with an electrolyte of LIPON, a cathode of V_2O_5 or $LiMn_2O_4$ and an anode of $Li_XV_2O_5$ deposited by RF sputtering. These thin-film batteries (Li-ion batteries) have the advantage of having a reduced complexity in manufacturing and an increased safety thus with a lithium anode. The Li-ion batteries disadvantage is the need to be charged before first use, which does not happen with the batteries with a lithium anode. The Baba *et al.* battery, displays an increased capability when it exceeds 20 cycles of charge/discharge reaching a maximum capacity of 10 µAh/cm^2 [32]. This behavior is attributed to the gradual decrease of resistance between the materials. Baba *et al.*, also proposed a higher battery voltage and higher current by stacking two batteries on the same substrate, allowing the reduction of the battery contacts. This battery operates at a voltage between 3 and 6.5 V and a current of 2 µA/cm^2 [33].

The development of thin-film batteries has almost 30 years of research, leading to the development of rechargeable lithium ion batteries. Table 3 shows some of the developed thin-film batteries.

TABLE 3: THIN-FILM BATTERIES [21].

Cathode	**Electrolyte**	**Anode**	**Voltage (V)**	**Current (µA/cm^2)**	**Capacity**	**Ref.**
TiS_2	$Li_{3,6}Si_{0,6}P_{0,4}O_4$	Li	2,5	16	45-150µAh/cm^2	[22]
TiS_XO_Y	Li_2SO_4-Li_2O-B_2O_3	Li	2,6	1-60	40-15µAh/cm^2	[34]
V_2O_5	LIPON	LiV_2O_5	3,5-3,6	10	6µAh/cm^2	[31]
$LiMn_2O_4$	LIPON	V_2O_5	3,5-1	>2	18µAh/cm^2	[32]
$LiMn_2O_4$	LiBP-LIPON	Li	3,5-4,5	70	100mAh/g	[35]
$LiMn_2O_4$	$Li_{6,1}V_{0,61}Si_{0,39}O_{5,36}$	Li	3,5-5	10	33,3µAh/cm^2	[25]
$LiMn_2O_4$	LIPON	Li	4,5-2,5	2-40	11-81µAh/cm^2	[36]
$LiCoO_2$	LIPON	Cu	4,2-3,5	1-5	130µAh/cm^2	[29]
$LiCoO_2$	LIPON	Li	4,2-2,0	50-400	35µAh/cm^2	[28]
$LiMn_2O_4$	LIPON	Li	4-5,3	10	10-30µAh/cm^2	[37]
Li-V_2O_5	LIPON	Li	1,5-3	2-40	10-20µAh/cm^2	[38]
$LiCoO_2$	LIPON	SiSnON	2,7-4,2	~5000	340-450mAh/g	[39]
$LiMn_2O_4$	LIPON	Li	4,3-3,7	~800	45µAh/(cm^2-µm)	[30]
$LiCoO_2$	$Li_{6.1}V_{0.61}Si_{0.39}O_{5.36}$	SnO	2,7-1,5	10-200	4-10µAh/cm^2	[40]

Thin-film batteries are available in the market by companies Cymbet [14] and Infinite Power Solutions [41]. Both use technology from ORNL, above. Four battery models are available from Cymbet:

- CBC012 (5 mm by 5 mm with a thickness of 0.9 mm)
- CBC050 (8 mm by 8 mm with a thickness of 0.9 mm)
- CBC3112 (7 mm by 7 mm with a thickness of 0.9 mm)
- CBC3150 (9 mm by 9 mm with a thickness of 0.9 mm)

The models CBC012 and CBC050 are also available with a package that allows connection to other integrated circuits (Fig. 4). CBC31xx models already include a load control and the ability to adjust the output voltage. Its technical characteristics can be found in Table 4. The Cymbet in conjunction with Texas Instruments also offers systems consisting of thin-film batteries and energy harvesting techniques.

5 mm x 5 mm DFN SMT Package

2.8 mm x 3.5 mm Bare Die

FIG. 4: THIN-FILM BATTERY CBC012 MARKETED BY CYMBET, AT RIGHT WITH ENCAPSULATION OF INTEGRATION WITH OTHER INTEGRATED CIRCUITS [14].

TABLE 4: TECHNICAL SPECIFICATIONS OF MARKED CYMBET BATTERIES.

Technical aspects	CBC012	CBC050	CBC3112	CBC3150
Output voltage (V)	3,8	3,8	3,3	3,3
Capacity (µAh)	12	50	12	50
Charge time (min)	30	50	30	50
Charge/discharge cycles	>5000	>5000	>5000	>5000

The Infinite Power Solutions also sells thin-film battery using $LiCoO_2$ as the cathode, the LIPON as electrolyte and metallic lithium as the anode. This provides, like Cymbet, four models of thin-film batteries. Its technical characteristics can be found in Table 5.

TABLE 5: TECHNICAL SPECIFICATIONS OF MARKED INFINITE POWER SOLUCTIONS BATTERIES

Technical aspects	MEC125	MEC120	MEC101	MEC102
Open voltage(V)	4,1	4,1	4,1	4,1
Internal resistance (Ω)	200	100	35	15
Capacity (mAh)	0,2	0,4	1	2,5
Charge time up to 90 % (min)	15	15	15	15
Life cycle (years)	>15	>15	>15	>15
Charge/discharge cycles	>10000	>10000	>10000	>10000
Self-discharge by year	<1%	<1%	<1%	<1%

2.3 MATERIALS FOR LITHIUM BATTERIES

Due to its characteristics, lithium is one of the most common materials used in solid-state batteries [21]. Lithium batteries are usually categorized by the anode material. Thus, batteries with metallic lithium anode are commonly known as "Li-Batteries". Batteries with anode of metal oxide or nitride are commonly known as "Li-ion Batteries" and batteries where the anode is also the current collector, usually copper, "Li-free Batteries".

In lithium batteries, the operating voltage is only defined by the chemical composition of battery cathode and anode and not by its size. Rather, the capacity is defined by the volume of battery cathode and anode. More volume means greater amount of lithium atoms, which results in a higher charge. During battery discharge, the operating voltage can go down a bit due to the battery's internal resistance.

Fig. 5 illustrates the discharge of a rechargeable battery with a cathode of lithium cobalt oxide ($LiCoO_2$) and lithium metallic anode. In the battery charge process is carried out the extraction of about 50 % of lithium from the cathode, which will be transferred to the anode. Lithium transferred will be used later in the discharge. However, considering the lithium anode, in the discharge will be transferred an even higher percentage of lithium. Chemical reactions of charge/discharge are shown in Table 6.

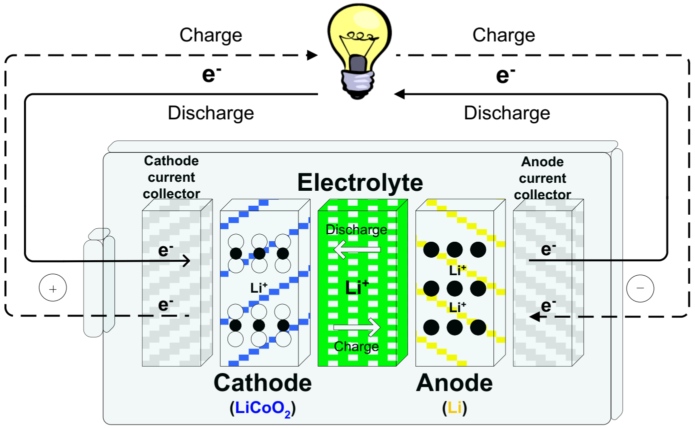

FIG. 5: RECHARGEABLE LITHIUM BATTERY WITH $LICOO_2$ CATHODE, WHERE THE EMPTY CIRCLES REPRESENT THE COBALT AND OXYGEN ATOMS AND THE FULL CIRCLES THE LITHIUM ATOMS.

TABLE 6: CHEMICAL REACTIONS OF CHARGE/DISCHARGE IN A RECHARGEABLE LITHIUM BATTERY.

Rechargeable lithium battery	
Charge	$LiCoO_2 = 0{,}5Li + Li_{0,5}CoO_2$
Discharge	$0{,}5Li + Li_{0,5}CoO_2 = LiCoO_2$

The separation between the battery cathode and anode is obtained through the electrolyte, which allows the passage of lithium ions, without letting pass lithium atoms or free electrons. Current collectors of cathode and anode only allow the passage of electrons. When an external circuit is connected to the battery, an oxidation reaction occurs at battery anode. This reaction will stimulate the electrons, though external circuit, and the ions, though the electrolyte, to flow to the battery cathode. The lithium ions move into the gaps created in the cathode during battery charge. The electrons and ions will recombine again in the battery cathode [4].

In Li-ion batteries the materials normally used as anode are SnO_2, $LiNiO_2$, $LiMn_2O_4$, V_2O_5, MoS_2, TiS_2 among others [42]. These materials must have the ability to accept large amounts of lithium ions. After battery fabrication the anode with these materials may not contain lithium, which restricts the choice of a cathode in a lithium-rich cathode, being the most common the $LiCoO_2$, the $LiMn_2O_4$ and the $LiNiO_2$.

The battery capacity or the amount of charges that can be provided are expressed in the amount of flowing current in a period of time (in hours), with the units Ah. How 1 A =1 Cs^{-1}, the battery capacity can also be expressed in Colombo (C), corresponding 1Ah to 3600 C.

The battery energy is given by its operating voltage multiplied by the loads supplied and is usually expressed in Wh. For example, a battery with an operating voltage of 4.2 V and a capacity of 50 μAh, provides an energy of 210 μWh. Contrary to the operating voltage, the battery energy depends of its size, since the amount of charge delivered is proportional to the cathode mass. The battery power supplied is its energy per unit time.

The energy and power per unit of volume or per unit of mass are often used to compare different battery technologies [21]. Fig. 6 compares lithium thin-film batteries, lithium polymer batteries and conventional batteries.

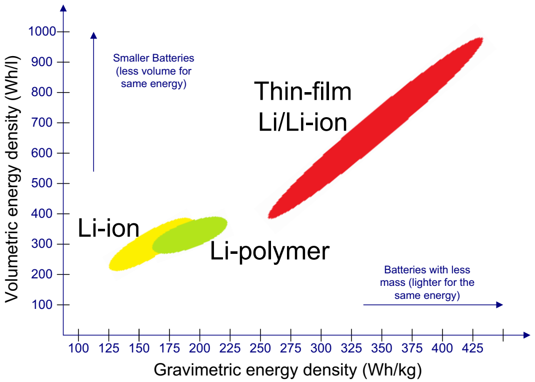

FIG. 6: BATTERIES COMPARISON OF VOLUMETRIC AND GRAVIMETRIC ENERGY DENSITY [21].

The battery volumetric energy density is calculated by dividing the power supplied to a specific discharge rate, by the total volume in litters, with the units Whl^{-1}. Rather, the battery gravimetric energy density is calculated by dividing the power supplied to a specific discharge rate, by the total mass in kilograms, with the units $Whkg^{-1}$.

The electrodes quality of a lithium ion battery has a high importance to its energy density [21]. The most important characteristics of an electrode in lithium-ion battery, which determine the energy that a battery can provide, are the number of electrons that the electrodes can store per unit volume or weight (volumetric and gravimetric energy density) and electrochemical potential they produce.

2.3.1 ANODES

The anode is the ion source of battery [2]. The oxidation reaction occurs in the anode, ions and electrons being released into the electrolyte and the external circuit, respectively. Ions supplied by anode diffuse into the electrolyte. The anode should be a light metal or light metal compound with low electronegativity (tendency of an atom to attract electrons in a chemical bond) and high electrical conductivity.

Lithium is an excellent choice as the anode of a battery due to its low molecular weight and low electronegativity [42]. The lithium metal, although the most common material in the anodes of solid-state batteries, has a melting temperature of 180.7 °C and is highly reactive with air. These reasons raise security issues in a battery. Table 7 compares other possible materials for battery anode in relation to capacity and present the major problem.

TABLE 7: ANODE MATERIAL COMPARATION [2].

Material (anode)	Capacity ($mAhg^{-1}$)	Problem
$Li_{21}Si_5$	1967	Volume change after first charge/discharge cycle
$Li_{22}Sn_5$	710	Volume change after first charge/discharge cycle
LiC_6	370	Limited capacity
InSb	270	Limited capacity
$CaSi_2$	320	Limited capacity
$Li_4Ti_5O_{12}$	168	Limited capacity
SiTON	450	Loss capacity after first charge/discharge cycle
SnO	1560	Loss capacity after first charge/discharge cycle

The materials for the anode shown in table above were investigated. These materials can't yet compete with lithium due to reduced capacity, changes in materials volume and high capacity loss after the first charge/discharge cycle.

2.3.2 CATHODES

The cathode of a lithium battery is where reduction reaction occurs by electron transfer [2]. During the battery discharge, electrons and ions are transferred from the anode to the cathode. To enable a rapid and effective transfer, the cathode must have a high electrical conductivity and high diffusivity and ion insertion capacity [42]. The higher open voltage of the cathode in relation to a reference, higher the operating voltage of the battery. The reference in lithium batteries is typically lithium metal. Table 8 compares some of the materials used as cathodes in lithium batteries, in relation to its theoretical gravimetric energy density and open voltage to metallic lithium.

TABLE 8: CATHODE MATERIALS COMPARATION [2].

Material (cathode)	Theoretical gravimetric energy density.($Whkg^{-1}$)	Open voltage in relation to metallic lithium (V)
TiS_2	473	2,1–2,5
V_2O_5	442	3-3,7
$LiCoO_2$	500	3,6-4,7
$LiMn_2O_4$	462	3-4,5

The preceding table indicates that the $LiCoO_2$ is the material that has better characteristics, both in gravimetric energy density or the voltage level. The $LiMn_2O_4$ also shows high gravimetric energy and voltage level, while the TiS_2 and V_2O_5 present with features considerably lower than others.

2.3.3 ELECTROLYTES

The electrolyte of a battery is essentially a passage for ions and a barrier to electrons or atoms without charge. Fundamental characteristics of an excellent electrolyte are a high ionic conductivity, high electrical resistivity, an excellent contact with the electrodes and an excellent chemical stability in contact with the electrodes [2].

In conventional batteries, the electrolyte is usually a liquid or an alkaline solution. This type of electrolyte, although it has high ionic conductivity, high electrical resistivity and an excellent contact with the cathode, requires an airtight and heavy package, which reduces the energy density and increases the battery size [21]. To reduce the size and increase the energy density of a battery, solid and glassy electrolyte is under investigation since 1970 [42]. Table 9 compares electrolytes materials in relation to their type and ionic conductivity.

TABLE 9: ELECTROLYTE MATERIALS COMPARATION [2].

Material (electrolyte)	Electrolyte type	Ionic conductivity (Scm^{-1})
$LiClO_4$ or $LiPF_6$ in EC-DEC/DMC and PC	Liquid	10^{-3}-10^{-2}
LiI	Solid	~$5,5x10^{-7}$
$Li_{0,33}La_{0,56}TiO_3$	Solid	10^{-4}
B_2O_3-xLi_2O-yLi_2SO_4 (x<0,6 e y<0,3)	Glassy	10^{-8}
xLi_2O-$ySiO_2$-zP_2O_5	Glassy	10^{-9}-10^{-7}
LIPON	Glassy	10^{-7}-10^{-6}

The preceding table indicates less ionic conductivity of glassy electrolyte than other types of electrolytes. However the. Glassy electrolytes are still quite advantageous in battery safety.

Polymer electrolytes (PEs) are complexes formed between ionic salts and polymers with electron-donor atoms, such as linear high molecular weight poly (oxyethylene) (PEO). These materials are in general divided into two groups: solid (or solvent-free) PEs (designated as SPEs) and gel polymer electrolytes [43].

SPEs were first introduced by Armand et al. [44] as an attractive alternative to non-aqueous liquid electrolytes in light-weight, rechargeable lithium batteries. The advantages of these materials include good electrochemical properties, a reduction in problems related to safety and environmental issues, and elimination of electrolyte leakage problems. These electrolytes may assume a multifunctional role as separator, adhesive and cell sealant in electrochemical devices. Li^+-based SPEs are considered to be attractive materials for application in electrochemical devices such as galvanic cells, electrochromic displays and sensors [45].

The most studied solid state polymer electrolyte (SPE) systems are based on poly(ethylene oxide), PEO, and are prepared by the dissolution of various guest ionic salts in the polymeric host matrix [46-50].

In spite of their technological potential, SPEs suffer from a series of drawbacks that have delayed their application in lithium batteries. These include a marked tendency to crystallize, substantially lower ionic conductivity (typically 10^{-8} to 10^{-5} Scm^{-1} at room temperature) than non-aqueous liquid electrolytes and a tendency for the ionic guest species to salt out at high salt concentration. As liquid electrolytes also pose significant safety and environmental concerns, in recent years considerable effort have been devoted to increasing the ionic conductivity and improving the mechanical properties of SPEs [43].

Unfortunately, the rather modest ionic conductivity of known systems continues to restrict the application of these materials as components in commercial products. In order to increase conductivity, different polymer matrix architectures [51], liquid plasticizing components [52, 53], ceramic fillers [54], plasticizing salts [55], as well as ionic liquids have been evaluated [56].

The most extensively investigated POE-based systems have included lithium salts [45], because of the foreseen applications in advanced primary and secondary batteries.

Lithium bis(trifluoromethanesulfone)imide ($LiN(SO_2CF_3)_2$, LiTFSI)-based PE systems [57-61] give on the average higher conductivities than other lithium salts [62]. This improvement of ionic conductivity is attributed to the low lattice energy of the salt, which facilitates the solvation of the lithium by the polymer, and to the deslocalized negative charge on the nitrogen and four oxygens atoms, which reduces ion pairing tendency. In addition, because of its shape and internal flexibility, the TFSI- anion exerts a plasticizing effect and reduces the crystallinity of the PE, therefore lowering the glass transition of the materials.

Several recent papers by Zhang et al. [63-65] have demonstrated that $LiBF_4$-based electrolytes are a good alternative to lithium hexafluorophosphate ($LiPF_6$)-based materials as components in low temperature Li-ion batteries with improved performance. These authors found that, although an electrolyte based on a solution of $LiBF_4$ in propylene carbonate/ethylene carbonate/ethylmethyl carbonate had lower ionic conductivity and a higher freezing temperature than the $LiPF_6$-based analogue, at –20 ºC the $LiBF_4$–based cell had lower charge-transfer resistance than the $LiPF_6$–based device. In spite of the slightly lower conductivity of the $LiBF_4$-based electrolyte, the cell based on this system showed slightly lower polarization and higher capacity in the liquid temperature range (above –20 ºC) of the electrolyte. These results suggested that the ionic conductivity of the electrolytes is not necessarily a limitation to the low-temperature performance of the Li-ion cell. The $LiBF_4$ salt may be a good choice for a low temperature electrolyte of a Li-ion cell if a solvent system that has low freezing temperature, high solubility towards $LiBF_4$, and good compatibility with a graphite anode can be formulated. Examples of SPEs doped with $LiBF_4$ and supporting acceptable levels of room temperature ionic conductivity have already been reported [66-70].

3 DEPOSITION AND CHARACTERIZATION TECHNIQUES

3.1 THIN-FILM DEPOSITION

The deposition of thin-films for current collectors, cathode, anode and electrolyte of battery was performed with the follow techniques:

- Thermal evaporation for anode;
- E-beam for current collectors;
- RF-Sputtering for cathode and electrolyte.

This thin-film deposition techniques bellow to the group denominated by Physical Vapour Deposition (PVD) [71]. The utilization of these techniques requires a controlled atmosphere being used in vacuum chambers, like in Fig. 7.

FIG. 7: VACUUM CHAMBER FOR PVD DEPOSITIONS.

3.1.1 THERMAL EVAPORATION

The thermal evaporation technique consists in the evaporation or sublimation of a material due to heating of the same [72]. When the material passes through the solid state for vapour state, without being liquid, sublimation occurs. Material creates vapours that after condensation in subtract, form a thin-film of the same material. The heater is achieved applying a high current in a crucible that contains the material to evaporate (Fig. 8). The standard crucibles are in tungsten, molybdenum or tantalum because they have high temperatures of evaporation/sublimation. The thermal evaporation technique intended to create a thin-film with the same composition of material placed in crucible [73].

FIG. 8: EXAMPLE OF SETUP FOR THERMAL EVAPORATION TECHNIQUE.

3.1.2 ELECTRON BEAM

Like thermal evaporation, e-beam is also a technique to evaporate/sublimate a determinate material over a heater of the same. This technique uses a high energy beam of electrons that focuses in material will provide the heater (Fig. 9) [74]. A magnetic field provides the targeting of electrons beam to material. The beams of electrons will focuses in a small area of material which prevent contamination [73] in comparison with thermal evaporation because is possible to reach higher temperatures. The Fig. 10 shows a setup for e-beam.

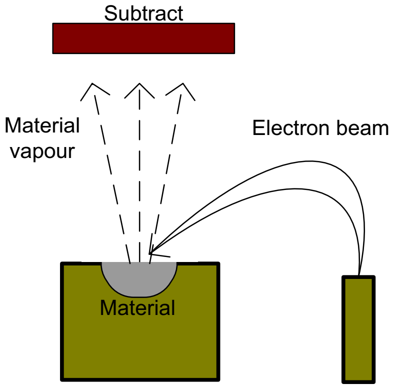

FIG. 9: WORKING DEMONSTRATION OF E-BEAM.

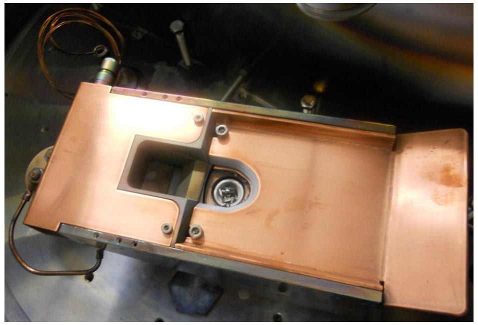

FIG. 10: EXAMPLE OF SETUP FOR E-BEAM.

3.1.3 SPUTTERING

The sputtering technique allows the deposition of thin-films at low temperature (typically less than 150 °C) [73]. The material to be deposited, denominated of target, is bombed with a beam of positive ions, that force the extraction of molecules/atoms of target surface. The beam of ions is achieved over the ionization and acceleration of a gas (normally argon) inside of the chamber [72]. The extracted molecules/atoms will form the thin-film on the subtract (Fig. 11). The sputtering technique allows the deposition of thin-films with better characteristics in terms of composition and uniformity [71], due to high area of incidence of ions beam on the target.

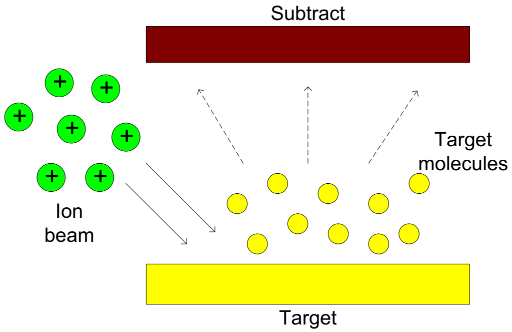

FIG. 11: **WORKING DEMONSTRATION OF SPUTTERING TECHNIQUE.**

The sputtering technique can be done by direct current (DC sputtering) or by radio frequency (RF sputtering). The DC sputtering is only applied in conductive materials, while the RF sputtering doesn't have that restriction [71]. The Fig. 12 shows a magnetron with a Li_3PO_4 target (used in electrolyte deposition).

FIG. 12: **MAGNETRON WITH LI_3PO_4 TARGET.**

3.2 MATERIAL CHARACTERIZATION

The thin-film characterization was performed using X-Ray Diffraction (XRD), Energy-Dispersive X-ray-spectroscopy (EDX) and Scanning Electron Microscope (SEM) techniques.

3.2.1 X-RAY DIFFRACTION

The XRD allows the quantification of crystalline structure of a given material. This technique is only possible because the atoms are usually ordered in crystal planes separated by distances of the same order of magnitude of the X-rays wavelength [75].

The phenomenon of diffraction occurs when an X-ray beam covers the crystal and interacts with the present atoms. The XRD is based on Bragg's Law (Equation 1) establishing the relationship between diffraction angle and the distance between the planes giving rise to (characteristic for each crystalline phase) [76].

$$n\gamma = 2d\sin\theta$$ **EQUATION 1**

Where:

- n is an entire number.
- γ is the wavelength of X-rays incident.
- d is the distance between the planes.
- θ is the diffraction angle.

When compared with others, the XRD technique is simple, fast and reliable. The possibility of analysis of materials composed of a mixture of phases and a quantitative analysis of these phases are the advantages of XRD.

3.2.2 DISPERSIVE X-RAYS SPECTROSCOPY AND ELECTRONIC SCAN MICROSCOPY

The EDX is an electron beam that focuses on a sample (which must be electrically conductive), causes excitation and removal of electrons from one orbit inside the material, creating a gap. The X-ray emission occurs when an electron from an outer orbit occupies the created gap. Chemical analysis of sample composition is possible because the wavelengths emitted are specific to each element of a material. The analysis is performed on all the material from the surface up to 2 µm depth and does not allow the composition of elements with a low atomic number (lithium for example).

The equipment composition by EDX analysis incorporates normally the microscope SEM. The SEM technique allows the achievement of an image of the surface material through the capture of electrons generated by a detection array [77].

3.3 OTHER PHYSICAL MEASUREMENTS ON THIN-FILMS BATTERIES

Beyond traditional characterizations for thin-films explained before, other physical measurements where performed, electrical resistivity, ionic conductivity, differential scanning calorimetry, thermal gravimetric analysis and cyclic voltammetry.

3.3.1 ELECTRICAL RESISTIVITY

The electrical resistivity was measured at four points (Fig. 13), using the Van der Pauw method [78].

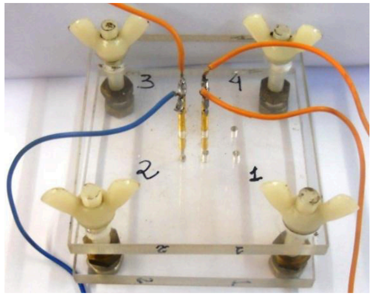

FIG. 13: SETUP FOR MEASURING RESISTIVITY.

The asymmetric configuration, the geometry of contact and the material anisotropy are corrected by repeating the measurement in four different configurations (Fig. 14). This technique of measuring at four points requires uniformity in the thickness of the sample [72].

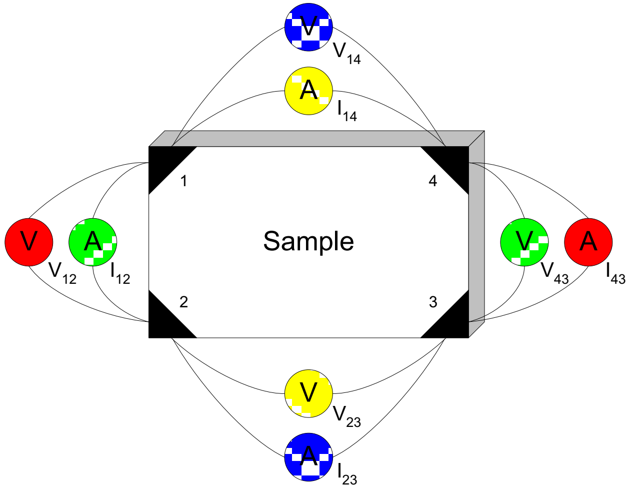

FIG. 14: SCHEMATIC OF EACH MEASURE NEEDED FOR THE RESISTIVITY MEASUREMENT.

The voltage drop is measured between two points while is applied a constant current intensity in the other two points. The voltage and current values are then used in Equation 2 and Equation 3, to calculate R_A and R_B, respectively.

$$R_A = \frac{V_{12}}{2I_{43}} + \frac{V_{43}}{2I_{12}} \qquad \text{EQUATION 2}$$

$$R_B = \frac{V_{14}}{2I_{23}} + \frac{V_{23}}{2I_{14}} \qquad \text{EQUATION 3}$$

Knowing R_A and R_B, and using the Equation 4 is calculated the value of R_S by numerical convergence.

$$e^{\left(-\pi\frac{R_A}{R_S}\right)} + e^{\left(-\pi\frac{R_B}{R_S}\right)} = 1 \qquad \text{EQUATION 4}$$

The value of resistivity is finally calculated with the value of R_S and the film thickness (h), as shown in Equation 5.

$$\rho = R_S h \qquad \text{EQUATION 5}$$

3.3.2 IONIC CONDUCTIVITY

The ionic conductivity is an important characterization parameter, which has been used as the criterion for quantification of electrolyte quality in lithium batteries. The ionic conductivity is a measure of the ions amount or ions clusters that can move through the action of an electrical or chemical potential [79].

In general, the ionic conductivity of the electrolytes is measured as a function of salt composition and temperature. The objective of this characterization is to identify the electrolyte with the most favourable behaviour for use as a component of the practical device.

Lithium batteries can have two different types of electrolytes. The solid electrolytes, that allows the fabrication of all battery by PVD techniques and the more common polymer electrolytes. A solid electrolyte and a polymer electrolyte (PE) intended for use in diverse electrochemical applications must have adequate ionic conductivity, together with negligible electronic conductivity if self-discharge on standing is to be avoided. A PE is considered to be a promising candidate for commercial application if its ionic conductivity is as high as 10^{-5} S cm^{-1} at room temperature [80, 81, 82].

In general, salts with a polarizing cation and a large anion with a well-delocalized charge, and therefore also with low lattice energy, are the most suitable for use in PEs [83, 84]. In spite of the dangers associated with the anion, lithium perchlorate ($LiClO_4$) is a salt that satisfies the conditions mentioned above. Lithium trifluoromethanesulfonate (or triflate) ($LiCF_3SO_3$) and $LiBF_4$ have also been extensively employed in this context [85]. Lithium bis(trifluoromethanesulfonyl)imide (LiTFSI) is particularly interesting as a guest species in solid PEs and also one of the best choices. In common with other salts that contain large polarizable anions, LiTFSI has low lattice energy and a low tendency to form ion-pairs, leading to enhanced ionic mobility. This salt also performs as a plasticizer in polyether electrolytes by creating free-volume. This is a significant advantage in polymer hosts that have an inherent tendency to crystallize.

Typically the total ionic conductivity of the electrolytes discussed here was measured by placing the sample between gold blocking electrodes, along the so-called *electrode/electrolytes/electrode assembly* (Fig. 15), which was secured in a suitable constant-volume support, to form a symmetrical cell. Low-amplitude alternating potentials at frequencies between 65 kHz and 0.5 Hz were applied over a range of temperatures from 20 to 80 ºC. This technique is possible, in an appropriate electrochemical system, due to separation of the analysis of the electrolyte response and the connections electrode/electrolyte response (Fig. 16).

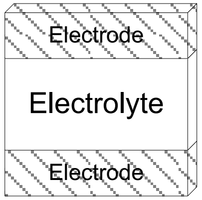

FIG. 15: SAMPLE FOR IONIC CONDUCTIVITY MEASURE.

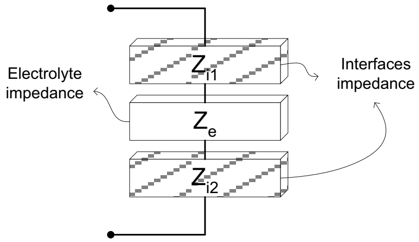

FIG. 16: IMPEDANCE OF SAMPLES FOR IONIC CONDUCTIVITY MEASURE [79].

The electrodes are typically in the form of reduced thickness disc, minimizing the separation distance between the electrodes and maximizing the area. This also allows the decreasing of electrical current that goes through the system which seeks to eliminate the possible change of electrochemical properties of the sample. These conditions guarantee the not transfer of electrical charge through the interface metal/electrolyte, due to these interfaces exhibit a purely capacitive behaviour. Whereas the interfaces electrode/electrolyte are equal, the equivalent circuit of Fig. 17 can be considered [86]. So for high frequencies, the impedance is dominated by the parallel circuit, corresponding to the electrolyte. For low frequencies, the impedance is dominated by the series circuit, predominantly interfaces electrode/electrolyte [87].

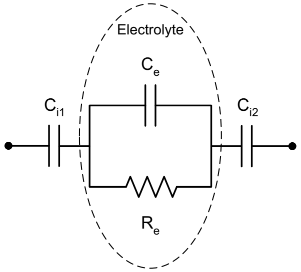

FIG. 17: EQUIVALENT CIRCUIT OF SAMPLE FOR IONIC CONDUCTIITY MEASURE [79].

The frequency spectrum is studied through the Nyquist diagram of the sample impedance. The Nyquist diagram is accomplished by applying a sinusoidal voltage to the sample in a high frequency range. Fig. 18 shows an example of a Nyquist diagram obtained with this technique. The figure shows that after tracing the Nyquist diagram, it is necessary to draw a semicircle to get the value $R(\Omega)$.

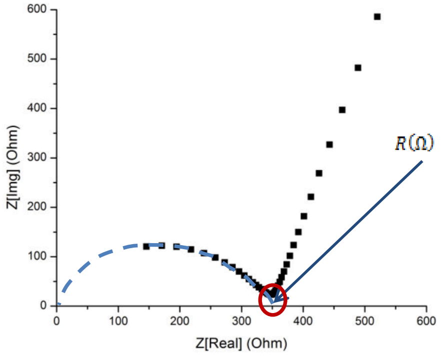

FIG. 18: EXAMPLE OF A NYQUIST DIAGRAM FROM AN ELECTROLYTE SAMPLE.

The R value is then applied in Equation 6, being h the film thickness, A the area and σ the ionic conductivity.

$$\sigma(Scm^{-1}) = \frac{h(\mu m)}{R(\Omega) * A(cm^2) * 10000}$$

EQUATION 6

3.3.3 THERMAL PROPERTIES

Thermal analysis techniques, in particular Differential Scanning Calorimetry (DSC) and Thermogravimetric Analysis (TGA), are valuable tools to study the thermal behaviour of electrolytes.

3.3.3.1 DIFFERENTIAL SCANNING CALORIMETRY (DSC)

The DSC is a technique of differential thermal analysis based on the release or absorption (depending on the material) of heat by the sample [88]. This technique characterizes the sample through the temperature difference between the sample itself and a reference material. The Fig. 19 represents a schematic illustration of DSC where one can see that the heating elements and temperature sensors of the sample and the reference are independent. The reference material is chosen to be inert and not subject to the release or absorption of heat in the temperature range investigated. This technique requires a chamber with temperature and atmosphere controlled. The atmosphere in the chamber is controlled by introducing an inert gas to clean the chamber prior to measurement and to protect the sample and prevent the deposition of ice on the inner surfaces of the chamber when operating at negative temperatures.

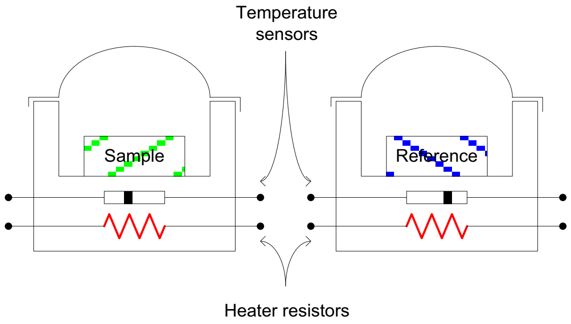

FIG. 19: SCHEMATIC REPRESENTATION OF DSC.

In case of PEs, DSC allows to calculate the proportion of crystallinity, to detect the formation of new crystalline phases, free guest salt or uncomplexed polymer chains, to monitor the loss of solvent(s) (*e.g.*, occluded water, alcohol), to determine the T_g value and to distinguish between endo- and exothermic events. For the DSC measurements of PEs samples, sections are usually subjected to thermal analysis under a flowing inert atmosphere between 25 and 300 ºC and at a heating rate of 5 ºC.min^{-1}.

Given the relative simplicity of construction, convenience in use and an adequate precision for most applications, the DSC is the preferred choice of manufacturers and thermal analysis techniques more common.

3.3.3.2 THERMAL GRAVIMETRIC ANALYSIS

The thermal analysis techniques are usually a group of techniques that registers a particular property of the sample as a function of temperature. In TGA technique is registered the weight of the sample as a function of temperature. The realization of this technique is based on the use of a thermal balance and requires a chamber with temperature and atmosphere controlled [88]. You need a prior knowledge of the mass of the sample at room temperature. The onset of thermal decomposition was estimated by extrapolation from TGA curves (Fig. 20). TGA provides rich information about the thermal degradation of the samples and their thermal stability domain.

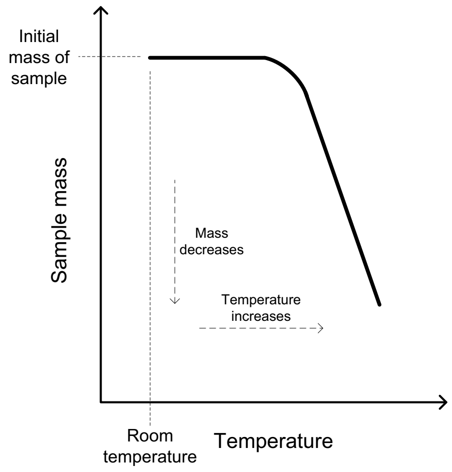

FIG. 20: TYPICAL GRAPH OF TGA.

3.4 CYCLIC VOLTAMMETRY

The application of the PEs in electrochemical applications depends on their stability window.

To evaluate the electrochemical stability window of PEs compositions we have typically used a two-electrode cell configuration involving the use of a 25 μm-diameter gold microelectrode surface. Cell assembly was initiated by locating a freshly-cleaned lithium disk counter electrode on a stainless steel current collector. A thin-film sample was centred over the counter electrode and the cell assembly completed by locating and supporting the microelectrode in the centre of the electrolyte disk. Measurements were conducted at room temperature within a Faraday cage.

The electrochemical stability range of the lithium-doped di-ureasils was determined by microelectrode cyclic voltammetry over the potential range between -1.5 and 6.5 V. In the anodic region, all electrolytes are stable up to 4.0 V *versus* Li/Li^+. Lithium deposition begins in the cathodic region at about -0.5 V *versus* Li/Li^+. These results support that the electrochemical stability of the PEs is acceptable for application in practical devices.

4 FABRICATION AND CHARACTERIZATION

4.1 ELECTRICAL CONTACTS

Platinum was the material chosen for the battery contacts for having high electrical conductivity, be inert in contact with the other battery materials and to allow a better distribution of electrons at the cathode surface. The platinum was deposited by e-beam technique. The integration of the battery manufacturing processes with integrated circuits is a very important aspect and therefore, the substrate must be compatible with these requests. The chosen substrate was silicon because it's the mostly used in manufacturing processes of integrated circuits [71].

A deposition of 100 nm of platinum was done for adhesion investigation. It appears that the adhesion of platinum to silicon is very vulnerable and the films were shown to be damaged. The resolution of this problem was achieved with the prior deposition of 30 nm of titanium [89-91], also using e-beam technique. This improved platinum adhesion and films were not damaged. After depositing the two materials is necessary to test their vulnerability to annealing, since this is necessary for the battery cathode. The sample was placed in an oven for two hours in vacuum at temperatures between 500 and 800 °C that is the same conditions necessaries for battery cathode. For these conditions of annealing, the films were not damaged, so the battery contacts are made of 30 nm of titanium and 70 nm of platinum (Fig. 21).

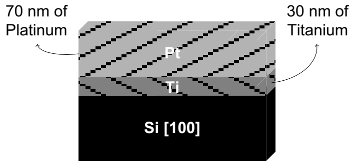

FIG. 21: BATTERY CONTACTS DEPOSITIONS.

4.2 CATHODE

The lithium cobalt oxide ($LiCoO_2$) was the chosen material for positive electrode (cathode) of the thin-film solid-state battery. The $LiCoO_2$ was chosen because of its excellent electrochemical stability and capacity of insertion and extraction of lithium ions. These characteristics derive from its excellent structural stability [92]. The most common material used in thin-film batteries is $LiCoO_2$, because it produces a high voltage [21, 93], and has a high performance over the cycles of charge/discharge (due to its structural stability, hold more than 500 cycles of charge/discharge maintaining its capacity by about 80 to 90%). Compared with other materials (for example, $LiMn_2O_4$ and $LiNiO_2$), the $LiCoO_2$ is easy to fabricate and can store a large amount of lithium ions. $LiCoO_2$ was deposited by RF sputtering, and deposition parameters can be found in Table 10. Films were deposited with different gases to adjust of fabrication process.

TABLE 10: CATHODE DEPOSITION PARAMETERS

Thin-film	**Deposition technique**	**Target**	**Thickness**	**Pressure**	**Supply power**	**Gas (sccm)**		
						O_2	Ar	N_2
#01	RF sputtering	$LiCoO_2$	1 μm	$2x10^{-3}$ mbar	150 W	10	30	-
#02						-	40	-
#03						-	40	-

After his deposition, LiCoO$_2$ was subjected to annealing [94, 95]. The annealing increased the crystallization and decreases the resistivity of the LiCoO$_2$ film, being carried out at temperatures between 500 and 800 °C. LiCoO$_2$ films annealing was performed in vacuum for two hours. Fig. 22 illustrates the deposition of LiCoO$_2$ to proceed to the annealing and after its characterization.

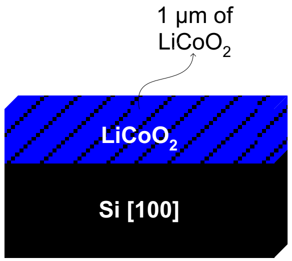

FIG. 22: BATTERY CATHODE ILLUSTRATION.

The thin-film characterization were performed by XRD techniques, Van de Pauw, EDX and SEM respectively to measure the crystallization, the electrical resistivity and chemical composition. Fig. 23 show the XRD patterns of LiCoO$_2$ films deposited for their annealing temperatures. Crystallographic analysis of the diffractograms was compared with the standard "016-0427" [96], which contains the crystal planes of LiCoO$_2$. In Fig. 23, the crystal planes that file are represented with lines (red) vertical. The spectra show the predominance of LiCoO$_2$ in the samples [97], especially in the sample "#03" (sample with better features). A detailed analysis allows us to observe that the crystal planes of LiCoO$_2$ increases with increasing of temperature to 700 °C. The plan [003], in particular, is one where denotes this additional feature, being one of the most important [97]. The annealing at 650 and 700 °C proved to be most suitable for obtaining a LiCoO$_2$ film. The crystal structure of LiCoO$_2$ film increases the diffusivity of lithium ion, which is a very important feature in the battery cathode.

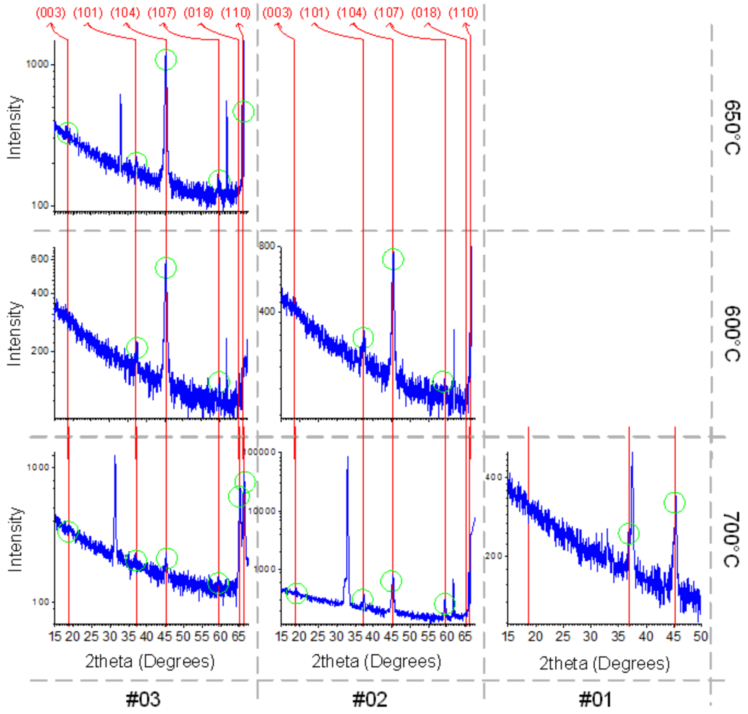

FIG. 23: XRD OF LIC$_O$O$_2$ FILMS WITH ANNEALING AT 700, 600 AND 650 °C. VERTICAL LINES (RED) CORRESPOND TO LIC$_O$O$_2$ PHASES AND CIRCUMFERENCES (GREEN) POINT THE CORRESPONDENCE PHASE IN SPECTRA.

The resistivity of LiCoO$_2$ films was measured by Van der Pauw technique. As can be seen in Fig. 24, the film subjected to an annealing of 650 °C under the conditions described above, was the film with better resistivity, about 3.7 Ωmm. The chemical composition of the film with improved resistivity was also analysed by EDX in Fig. 25. Note that the atomic number of lithium is quite small, and therefore not covered by this technique. A SEM image was also performed (Fig. 26), where denotes the formation of crystals in the LiCoO$_2$ film surface.

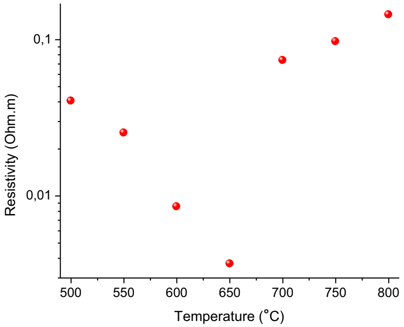

FIG. 24: LICOO$_2$ FILMS RESISTIVITY FROM DEPOSITION "#03".

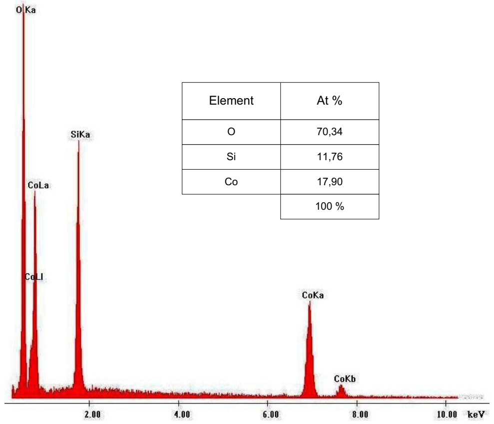

Element	At %
O	70,34
Si	11,76
Co	17,90
	100 %

FIG. 25: LICOO$_2$ FILM CHEMICAL COMPOSITION.

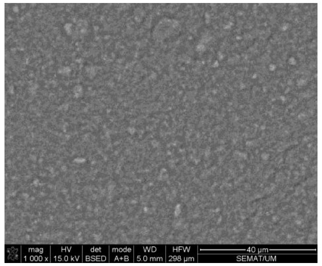

FIG. 26: LICOO$_2$ FILM SEM, SURFACE PICTURE.

4.3 ELECTROLYTE

The main features of electrolyte are a high ionic conductivity, high electrical resistivity and be stable in contact with cathode and anode of the battery [21]. It is generally accepted that amorphous materials (without crystal planes) have a higher ionic conductivity [98]. These characteristics are met by the lithium phosphorus oxynitride (LIPON), which is the chosen material for electrolyte of thin-film solid-state battery. The LIPON also has a high electrochemical stability, which drives its use in thin-film batteries [99]. An electrical resistivity greater than 10^{14} Ωcm is also an important feature of LIPON, because it prevents the self-discharge of battery, increasing the time it keeps the battery charged [100]. The LIPON was deposited by RF sputtering and the deposition parameters can be found in Table 11. Pressure was kept at different values during the deposition of each film to correlate the deposition parameters with film properties.

TABLE 11: ELECTROLYTE DEPOSITION PARAMETERS

Thin-film	Deposition technique	Target	N_2	Pressure	Power supply	Thickness
#01	RF sputtering	Li_3PO_4	20 sccm	$1x10^{-2}$ mbar	200 W	1 µm
#02				$2x10^{-3}$ mbar		
#03				$7x10^{-3}$ mbar		
#04				$3x10^{-4}$ mbar		
#05				$3x10^{-4}$ mbar	150 W	

Fig. 27 illustrates the deposition of LIPON films to measure the ionic conductivity. The aluminium substrate was chosen because of its high electrical conductivity and low cost, being used as a contact. To improve contact, LIPON was deposited between platinum films. Subsequently, an aluminium disk with a diameter less than the substrate (to ensure non-occurrence of short circuit) was glued (using silver glue) at the top of the sample to ensure its robustness (Fig. 28).

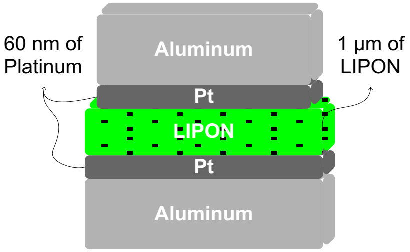

FIG. 27: ELECTROLYTE DEPOSITION ILLUSTRATION.

FIG. 28: LIPON SAMPLE WITH UPPER AND LOWER CONTACT.

The ionic conductivity was measured by applying a sinusoidal voltage with 25 mV peak to peak to the sample in a range of frequencies between 0.5 Hz and 65 kHz. Reading the response of the sample allowed drawing the Nyquist diagram of the sample impedance [98, 101]. Fig. 29 illustrates examples of the Nyquist diagrams for the sample "#4" and "#5" at different temperatures.

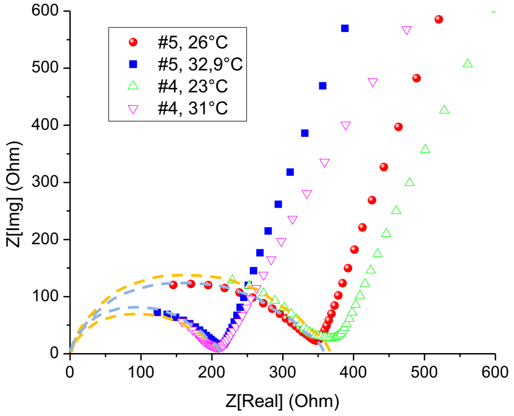

FIG. 29: NYQUIST DIAGRAM OF LIPON FILMS.

Semicircles in Nyquist diagram (Fig. 29) was traced with the help of a specific program (in this work was used Autolab). The intersection of the semicircle with the x-axis indicates the resistance value to be applied in the formula of ionic conductivity (Equation 6). In Fig. 30 shows the value of ionic conductivity for the various depositions parameters (Table 11). Please note that ionic conductivity increases with increasing temperature. The reduction of pressure and power source during the deposition increases the ionic conductivity. The graph of Fig. 31 shows the ionic conductivity of depositions "1", "3" and "4" in function of pressure during deposition.

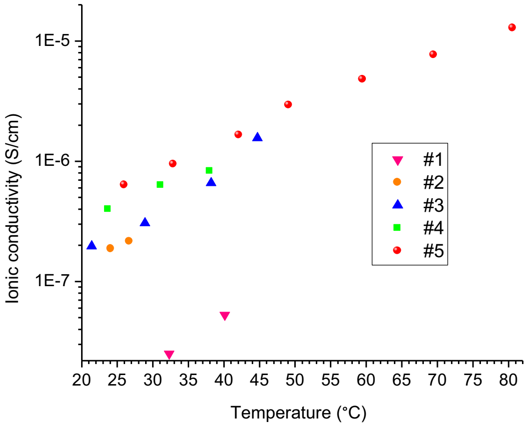

FIG. 30: IONIC CONDUCTIVITY OF LIPON FILMS.

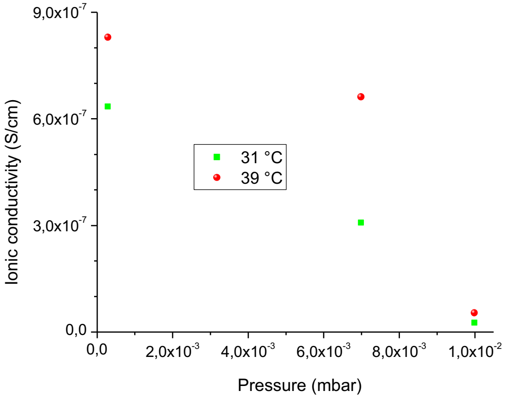

FIG. 31: IONIC CONDUCTIVITY OF LIPON FILMS IN FUNCTION OF PRESSURE DURING DEPOSITION.

The ionic conductivity of the sample "#4" was also measured after being exposed to the ambient atmosphere for a month (Fig. 32). It was concluded that the behaviour of the sample remained, but its ionic conductivity decreased considerably.

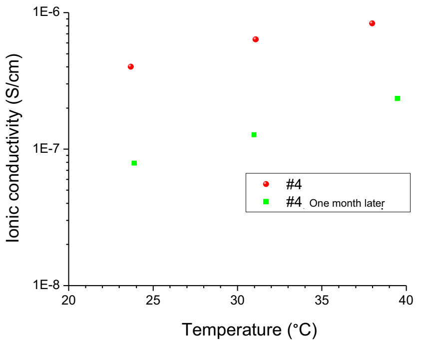

FIG. 32: COMPARISON OF LIPON IONIC CONDUCTIVITY ONE MONTH LATER AT AIR ESPOSURE.

The chemical composition of LIPON film was also measured using EDX technique, where the oxygen has the largest share of atomic percentage (Fig. 33). Images of the surface and cut of LIPON samples were also performed by SEM technique (Fig. 34). Note that the images do not show crystalline grains. The XRD analysis also confirmed the amorphous structure.

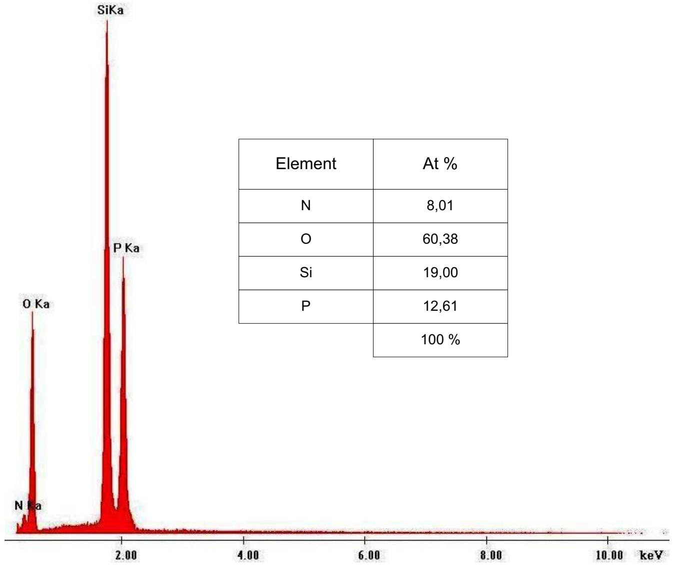

Element	At %
N	8,01
O	60,38
Si	19,00
P	12,61
	100 %

FIG. 33: EDX OF LIPON FILM.

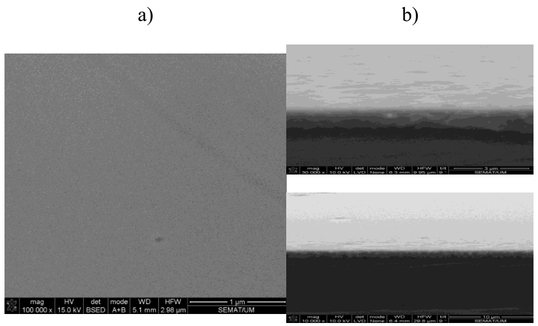

FIG. 34: LIPON SEM, A) SURFACE PICTURE, B) CUT IMAGES.

The thermal stability of LIPON films was also measured by Differential Scanning Calorimetry (DSC) and Themogravimetric analysis (TGA) techniques. Fig. 35 shows the result obtained with DSC and Fig. 36 shows the result obtained from the TGA. Through these graphs is concluded that the LIPON is stable when subjected to temperatures up to 400 °C.

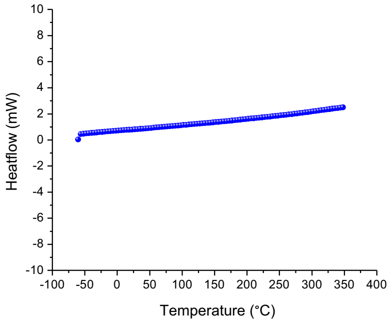

FIG. 35: HEATFLOW (MW) OF LIPON FILM IN FUNCTION OF TEMPERATURE DURING DSC ANALYSIS.

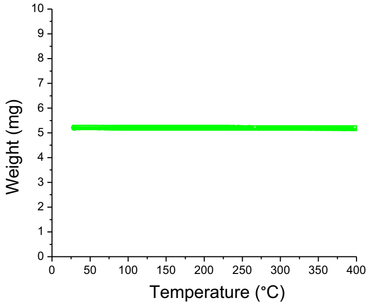

FIG. 36: WEIGHT OF LIPON FILM IN FUNCTION OF TEMPERATURE DURING TGA ANALYSIS.

4.4 ANODE

Initially, the lithium metal was the material chosen as the anode (negative electrode) of thin-film solid state battery. This material was chosen due to the large amount of lithium ions that can provide during battery discharge. Contacts were deposited on glass to make the measurement of resistance within the vacuum chamber and during deposition. Lithium was deposited by thermal evaporation and deposition parameters can be found in Table 12.

TABLE 12: DEPOSITION PARAMETERS OF ANODE.

Thin-film	Deposition technique	Current source	Thickness	Resistance with 3 µm thickness
#01	Thermal evaporation	150 A	6 µm	3,26 Ω
#02			5,3 µm	3,04 Ω
#03			3,3 µm	3,5 Ω

The last column of the table above shows the resistance value measured when the lithium film reaches 3 µm thick. The graph of Fig. 37 shows resistance values measured during depositions. The resistance measurements were performed during the deposition with a four point setup.

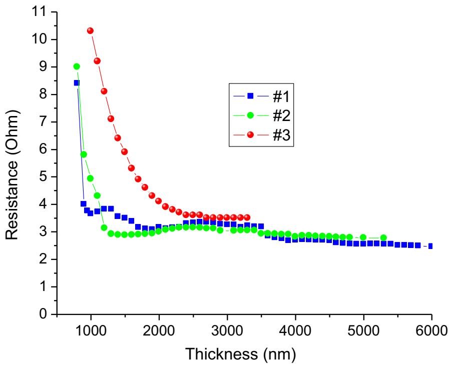

FIG. 37: LITHIUM RESISTANCE DURING DEPOSITION.

After deposition, was investigated the resistance of lithium when it comes into contact with atmosphere. The results in Fig. 38 show that lithium film oxidizes very quickly in contact with the ambient atmosphere and thus a protective film, deposited on top of lithium, is essential for battery functioning.

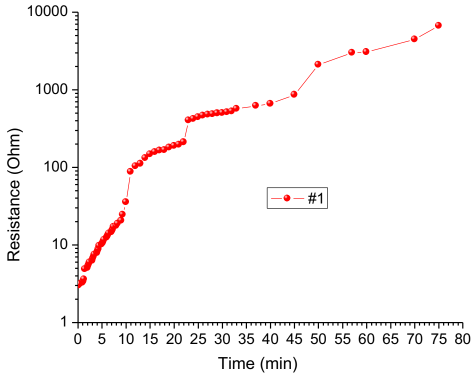

FIG. 38: LITHIUM RESISTANCE MEASURED DURING AMBIENT ATMOSFHERE EXPOSURE.

4.5 BATTERY FABRICATION

The fabrication of solid-state lithium battery was projected using only shadow masks. The shadow masks are essential for fabrication of battery to prevent short circuit between battery electrodes due to lack of lithography processes that can replace the shadow masks. The shadow mask to the battery current collectors allows that contacts have the format shown in Fig. 39. The cathode current collector is on the left side of the image and the anode current collector on the right side.

FIG. 39: DESIGN OF BATTERY CURRENT COLLECTORS (THICKNESS WAS EXAGERATED FOR BETTER VISUALIZATION).

Then, the battery cathode is deposited as illustrated in Fig. 40, being connected only with the cathode current collector. This takes into account the area needed to connect an electric wire (left margin on the left).

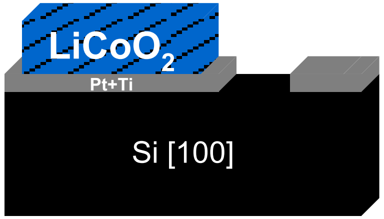

FIG. 40: DESIGN OF BATTERY CATHODE (THICKNESS WAS EXAGERATED FOR BETTER VISUALIZATION).

After $LiCoO_2$ annealing, the electrolyte deposition is performed as shown in Fig. 41. The electrolyte fills the gap left by the previous mask to ensure isolation between cathode and anode of battery.

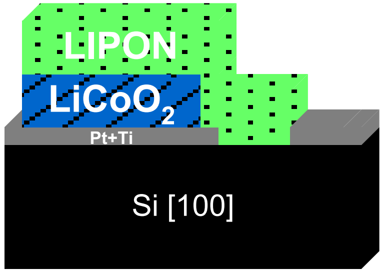

FIG. 41: DESIGN OF BATTERY ELECTROLYTE (THICKNESS WAS EXAGERATED FOR BETTER VISUALIZATION).

The battery manufacture is completed with the deposition of anode, as shown in Fig. 42. Fig. 42 also indicates positive and negative battery contacts. Note that without a protective film deposited over the battery anode it cannot operate outside the vacuum chamber.

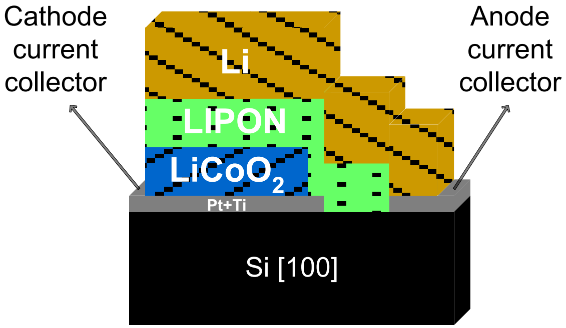

FIG. 42: DESIGN OF COMPLETE BATTERY (THICKNESS WAS EXAGERATED FOR BETTER VISUALIZATION).

5 CONCLUSIONS

The overall objective of this work was to select, fabricate and characterize the materials to fabricate a lithium solid-state battery. A lithium battery is composed primarily of three materials, cathode, electrolyte and anode. The manufacturing process and design for battery was projected. The results presented in this work fall within the above objectives, presenting the following solutions:

- ✓ Silicon substrate, to integrate the battery with microelectronics processes.
- ✓ Current collectors consisting of two thin-films, 30 nm titanium and 70 nm platinum. With this solution was eliminated the adhesion problem of platinum to silicon. Unwanted reactions between the contacts and the electrodes are prevented by using platinum.
- ✓ Cathode (positive electrode) of lithium cobalt oxide ($LiCoO_2$) with a fully crystalline structure and high capacity of insertion/extraction of lithium ions.
- ✓ Electrolyte of lithium phosphorus oxynitride (LIPON) with high ionic conductivity and stable up to 400 °C.
- ✓ Anode (negative electrode) of metallic lithium, which allows a high amount of lithium ions.
- ✓ Manufacturing process with different structures for each of the constituent materials of the battery, preventing contact between battery electrodes. Manufacture of films using shadow masks, due to lithography processes are not yet developed to the chosen materials.

LiCoO$_2$

The $LiCoO_2$ is mostly used as cathode material in lithium batteries due to its excellent electrochemical stability, high capacity of lithium-ion diffusion and provide a high voltage to the battery. The fully crystalline structure facilitates the diffusivity of lithium ions and decreases the resistivity of the $LiCoO_2$. The $LiCoO_2$ film was deposited by RF sputtering and presented the best characteristics with a power source of 150 W, a pressure of $2x10^{-3}$ mbar, 40 sccm of argon and an annealing at 650 °C for two hours in vacuum. Electrical resistivity of 3.7 Ωmm was achieved and chemical composition proven by EDX technique. A SEM image was also show the crystallization of $LiCoO_2$ film.

LIPON

LIPON is a glassy electrolyte and must have a high ionic conductivity and high electrical resistivity. It has an electrical resistivity greater than 10^{14} Ω and has an ionic conductivity of $6.3x10^{-7}$ Scm^{-1} for a temperature of 26 °C. The LIPON was deposited by RF sputtering with a power source of 150 W, pressure of $3x10^{-4}$ mbar and 20 sccm of nitrogen. The chemical composition and structure of the amorphous LIPON were proven using the EDX and SEM techniques. Thermal stability of LIPON up to 400 °C was also proven using the DSC and TGA techniques.

Lithium

The lithium metal is the most common material used as battery anode due to the high amount of lithium ions that can provide to battery discharge. This was deposited by thermal evaporation and its resistance measured during the deposition. The resistance of about 3.5 Ω was measured and the oxidation of the film in contact with the ambient atmosphere evaluated. The necessity of a protective film was proved to prevent oxidation of lithium.

5.1 FUTURE TRENDS FOR THIN-FILM BATTERIES

The fabrication and characterization of a battery, using the process presented and optimized manufacturing revenues during this work will provide the desired goal in this area: a rechargeable solid-state battery, totally fabricated in thin-films. The battery characterization must be placed within the vacuum chamber to prevent oxidation. Then, a material that protects the battery from the oxidation must be found and tested. It is suggested the use of LIPON, silicon nitride or Parylene as protection layer. The substitution of metallic lithium as anode of battery by a material having a melting point higher will allow the welding processes on the battery. On the other hand, the use of nano-structured materials at the anode and cathode opens horizons for the development of batteries with times of charge/discharge of tens of seconds. The integration of the battery in microelectronics manufacturing processes would be the next step, aiming at their integration in integrated circuits.

REFERENCES

[1] T. Minami, *et al.*, “*Solid state ionics for batteries*”, Spinger, 2005.

[2] Nava Ariel, “*Integrated thin film batteries on silicon*”, Phd thesis, Massachusetts Institute of Technology, 2005.

[3] K. Xu, “*Nonaqueous Liquid Electrolytes for Lithium-Based Rechargeable Batteries*”, Chemical Reviews, vol. 104, 2004, 4303-4417.

[4] F. S. Spear, “*The quantitative relationships among P, T, chemical potential, phase composition and reaction progress in igneous and metamorphic systems*”, Mineralogy and Petrology, vol. 99, 1988, 249-256.

[5] A. Volta, “*On the electricity excited by the mere contact of conducting substances of different species*”, Philosophical Trans. Royal Society, 1800.

[6] I. Buchmann, “*Batteries in a portable world*”, Cadex Electronics Inc., 1997.

[7] P. Gallone, “*Galvani's frog: Harbinger of a new era*”, Electrochimica Acta, vol. 31, 1986, 1485-1490.

[8] M. Piccolino, “*The bicentennial of the voltaic battery (1800-2000): the artificial electric organ*”, Perspectives, vol. 23, 2000, 147-151.

[9] http://www.mpoweruk.com/history.htm, consulted at 23-09-2011.

[10] http://www.energizer.eu, consulted at 23-09-2011.

[11] R. Moshtev and B. Johnson, “*State of the art of commercial Li ion batteries*”, Journal of Power Sources, vol. 91, 2000, 86-91.

[12] Y. Nishi, “*Lithium ion secondary batteries; past 10 years and the future*”, Journal of Power Sources, vol. 100, 2001, 101-106.

[13] K. Murata, *et al.*, “*An overview of the research and development of solid polymer electrolyte batteries*”, Electrochimica Acta, vol. 45, 2000, 1501-1508.

[14] http://www.cymbet.com/products/index.php, consulted at 23-09-2011.

[15] M. Armand and J. Tarascon, “*Building better batteries*”, Nature, vol. 451, 2008, 652-657.

[16] A. S. Aricò, *et al.*, “*Nanostructured materials for advanced energy conversion and storage devices*”, Nature Materials, vol. 4, 2005, 366-377.

[17] L. F. Nazar, *et al.*, “*Nanostructured materials for energy storage*”, International Journal of Inorganic Materials, vol. 3, 2001, 191-200.

[18] P. G. Bruce, *et al.*, “*Nanomaterials for rechargeable lithium batteries*” Angewandte Chemie International Edition, vol. 47, 2008, 2930-2946.

[19] Wei-Yang Li, *et al.*, “Co_3O_4 *nanomaterials in lithium-ion batteries and gas sensors*”, Advanced Functional Materials, vol. 15, 2005, 851-857.

[20] H. Chen, *et al.*, “*From biomass to a renewable* $Li_XC_6O_6$ *organic electrode for sustainable Li-ion batteries*”, ChemSusChem, vol. 1, 2008, 348-355.

[21] A. Patil, *et al.*, “*Issue and challenges facing rechargeable thin film lithium batteries*”, Materials Research Bulletin, vol. 43, 2008, 1913-1942.

[22] K. Kanehori, *et al.*, “*Thin film solid electrolyte and its application to secondary lithium cell*”, Solid State Ionics, vol. 9-10, 1983, 1445-1448.

[23] I. E. Kelly, *et al.*, “*Poly(ethylene oxide) electrolytes for operation at near room temperature*”, Journal of Power Sources, vol. 14, 1985, 13-21.

[24] H. Ohtsuka and J. Yamaki, “*Preparation and Electrical Conductivity of Li2O-V2O5-SiO2 thin films*”, Journal of Applied Physics, vol. 28, 1989, 2264-2267.

[25] H. Ohtsuka, *et al.*, “*Solid state battery with* Li_2O-V_2O_5-SiO_2 *solid electrolyte thin film*”, Solid State Ionics, vol. 40-41, 1990, 964-966.

[26] M. M. Mojarradi, *et al.*, “*Power management and distribution for system on a chip for space applications*”, Jet Propulsion Laboratory, California Institute of technology, n.º 284.

[27] X. Yu, *et al.*, “*A stable thin-film lithium electrolyte: lithium phosphorus oxynitride*”, Journal of Electrochemical Society, vol. 144, 1997, 524-532.

[28] B. Wang, *et al.*, “*Characterization of thin-film rechargeable lithium batteries with lithium cobalt oxide cathodes*”, Journal of Electrochemical Society, vol. 143, 1996, 3203-3213.

[29] B. J. Neudecker, *et al.*, “*”Lithium-free” thin-film battery with in situ plated Li anode*”, Journal of Electrochemical Society, vol. 147, 2000, 517-523.

[30] Y. S. Park, *et al.*, “*All-solid-state lithium thin-film rechargeable battery with lithium manganese oxide*”, Electrochemical Solid-State Letters, vol. 2, 1999, 58-59.

[31] M. Baba, *et al.*, “*Fabrication and electrochemical characteristics of all-solid-state lithium-ion batteries using* V_2O_2 *thin films for both electrodes*”, Electrochemical Solid-State Letters, vol. 2, 1999, 320-322.

[32] M. Baba, *et al.*, “*Fabrication and electrochemical characteristics of all-solid-state lithium-ion rechargeable batteries composed of* $LiMn_2O_4$ *positive and* V_2O_5 *negative electrodes*”, Journal of Power Sources, vol. 97-98, 2001, 798-800.

[33] M. Baba, *et al.*, “*Multi-layered Li-ion rechargeable batteries for a high-voltage and high-current solid-state power source*”, Journal of Power Sources, vol. 119-121, 2003, 914-917.

[34] G. Meunier, *et al.*, “*New positive-electrode materials for lithium thin film secondary batteries*”, Materials Science and Engineering: B, vol. 3, 1989, 19-23.

[35] S. S. Zhang, “*The effect of the charging protocol on the cycle life of a Li-ion battery*”, Journal of Power Sources, vol. 161, 2006, 1385-1391.

[36] N. J. Dudney, *et al.*, “*Nanocrystalline* Li_XMn_2-YO_4 *cathodes for solid-state thin-film rechargeable lithium batteries*”, Journal of Electrochemical Society, vol. 146, 1999, 2455-2464.

[37] J. B. Bates, *et al.*, “*5 volt plateau in* $LiMn_2O_4$ *thin films*”, Journal of Electrochemical Society, vol. 142, 1995, L149-L151.

[38] J. B. Bates, *et al.*, “*Thin-film rechargeable lithium batteries*”, Journal of Power Sources, vol. 54, 1995, 58-62.

[39] B. J. Neudecker, *et al.*, “*Lithium silicon tin oxynitride* (Li_YSiTON)*: high-performance anode in thin-film lithium-ion batteries for microelectronics*”, Journal of Power Sources, vol. 81-82, 1999, 27-32.

[40] S. D. Jones and J. R. Akridge, “*A thin film solid state microbattery*”, Solid State Ionics, vol. 53-56, 1992, 628-634.

[41] http://www.infinitepowersolutions.com/, consulted at 23-09-2011.

[42] J. O. Besenhard, “*Handbook of battery materials*”, Wilcy-VCH, 1999.

[43] F. M. Gray, “*Solid Polymer Electrolytes: Fundamentals and Technological Applications*”, VCH Publishers, New York, 1991.

[44] M. Armand, *et al.*, “*Extended Abstracts Second International Conference on Solid Electrolytes*”, St Andrews, Scotland, 1978.

[45] J.-M. Tarascon and M. Armand, “*Issues and challenges facing rechargeable lithium batteries”* Nature, vol. 414, 2001, 359.

[46] F. M. Gray, “*Polymer Electrolytes, RSC Materials Monographs*”, Royal Society of Chemistry, London, 1997.

[47] D.E. Fenton, *et al.*, “*Complexes of alkali metal ions with poly (ethylene oxide)*”, Polymer, vol. 14, 1973, 589.

[48] P.G. Bruce (Ed.), “*Solid-state electrochemistry*”, Cambridge University Press, Cambridge, 1995.

[49] P. M. Blonsky, *et al.*, “*Polyphosphazene solid electrolytes*”, J. Am. Chem. Soc., vol. 106, 1984, 6854-6855.

[50] J. R. MacCallum and C. A. Vincent (Eds), “*Polymer Electrolytes Reviews*”, Elsevier Applied Science, London, 1987, 1-22.

[51] R. Frech and S.Chintapalli, “*Effect of propylene carbonate as a plasticizer in high molecular weight PEO□LiCF3SO3electrolytes*”, Solid State Ionics, 1996, 85-61.

[52] M. M. Silva, *et al.*, “*Study of novel lithium salt-based, plasticized polymer electrolytes*”, J Power Sources, 2002, 52-57.

[53] M. M. Silva, *et al.*, “*Characterization of a novel polymer electrolyte based on a plasticizing lithium salt*”, in Advanced Batteries and Super Capacitors, Eds., G. Nazri, R. Koetz, B. Scrosati, P. A. moro and E. S: Takeuchi, The Electrochemical Society Proceedings Series PV2001-21, 2003, 476.

[54] CW Walker and M. Salomon, “*Improvement of Ionic Conductivity in Plasticized PEO-Based Solid Polymer Electrolytes*”, J Electrochem Soc, vol. 140, 1993, 3409.

[55] F. Alloin, *et al.*, “*Conductivity measurements of LiTFSI triblock copolymers with a central POE sequence*”, Electrochim Acta, vol. 37, 1992, 1729.

[56] A. L. Pont, *et al.*, “*Pyrrolidinium-based polymeric ionic liquids as mechanically and electrochemically stable polymer electrolytes*”, J Power Sources, 2009, 558-563.

[57] M. Armand, *et al.*, In Second International Symposium on Polymer Electrolytes; B. Scrosati, Ed.; Elsevier Applied Science, New York, 1990, 91.

[58] W. Gorecki, *et al.*, “*Physical properties of solid polymer electrolyte PEO(LiTFSI) complexes*”, Phys. Condens. Matter, vol. 7, 1995, 6823.

[59] A. Vallée, *et al.*, "*Comparative study of poly(ethylene oxide) electrolytes made with LiN(CF3SO2)2, LiCF3SO3 and LiClO4: Thermal properties and conductivity behaviour*", J. Electrochim. Acta, vol. 37, 1992, 1623.

[60] M. Hernandez, *et al.*, "*Spectroscopic characterization of metal chloride/polyamide complexes*", Ionics, vol. 1, 1995, 454.

[61] S. Lascaud, *et al.*, "*Phase diagrams and conductivity behavior of poly (ethylene oxide)-molten salt rubbery electrolytes*", Macromolecules, vol. 27, 1994, 7469.

[62] F. Gray, "*Polymer Electrolytes*", RSC Materials Monographs, The Royal Society of Chemistry, London, 1997.

[63] S. S. Zhang, *et al.*, "*Understanding Formation of Solid Electrolyte Interface Film on* $LiMn_2O_4$ *Electrode*", J. Electrochem. Soc. vol. 149, 2002, A586.

[64] S. S. Zhang, *et al.*, "*A new approach toward improved low temperature performance of Li-ion battery*", Electrochem. Comm., vol. 4, 2002, 928.

[65] S. S. Zhang, *et al.*, "*Low-temperature performance of Li-ion cells with a* $LiBF_4$*-based electrolyte*", J. Solid State Electrochem., vol. 7, 2003, 147.

[66] P. C. Barbosa, *et al.*, "*Phase relationships and conductivity of the polymer electrolytes poly(ethylene oxide)/lithium tetrafluoroborate and poly(ethylene oxide)/lithium trifluoromethanesulfonate*", J. Mater. Chem., vol. 20, 2010, 723.

[67] S. M. Zahurak, M. L. Kaplan, E. A. Rietman, D. W. Murphy, R. J. Cava, Macromolecules 21 (1988) 654.

[68] M. M. Silva, *et al.*, "*Characterization of solid polymer electrolytes based on poly(trimethylenecarbonate) andlithium tetrafluoroborate*", Electrochim. Acta, vol. 49, 2004, 1887.

[69] G. Chiodelli, *et al.*, "*Ionic conduction and thermal properties of PEO-lithium tetrafluoro borate films*", Solid State Ionics, 1988, 1009.

[70] M. B. Armand, *et al.*, "*Fast Ion Transport in Solids*", Elsevier, Amsterdam, 1979, 131-136.

[71] José Higino Correia and João Paulo Carmo, "Introdução às microtecnologias no silício", LIDEL, 2010.

[72] Aicha A. R. Elshabini-Riad and Fred D. Barlow III, "*Thin film technology handbook*", McGraw-Hill Companies, 1998.

[73] Nadim Maluf, "*An introduction to microelectromechanical systems engineering*", Artech House, 2000.

[74] Stephen A. Campbell, "*The science and engineering of microelectronic fabrication*", Oxford University Press, 2001.

[75] Luís Gonçalves, "Microssistema termoeléctrico baseado em teluretos de bismuto e antimónio", Phd Thesis, University of Minho, 2008.

[76] B. D. Cullity and S. R. Stock, "*Elements of X-ray diffraction*", Addison – Wesley, 1978.

[77] http://www.purdue.edu/rem/rs/sem.htm, consulted at 23-09-2011.

[78] L. J. van der Pauw, "*A method of measuring the resistivity and Hall coeficiente on lamellae of arbitrary shape*", Philips Technical Review, vol. 20, 1958, 220-224.

[79] Carlos Silva, "*Preparação e caracterização de electrólitos poliméricos*", Phd Thesis, University of Minho, 1996.

[80] C. R. A. Catlow, *et al.*, "*An EXAFS study of the structure of rubidium polyethyleneoxide salt complexes*", Solid State Ionics, vol. 9-10, 1983, 1107-1113.

[81] P. G. Bruce, *et al.*, "*Preliminary Results on a New Polymer Electrolyte PEO-Hg(*ClO_4*)2*", Br Polym J, vol. 20, 1988, 193-194.

[82] Armstrong R D and Clarke M D, "*Lithium ion conducting polymeric electrolytes based on poly(ethylene) adipate*", Electrochim Acta, vol. 29, 1984, 1443-1446.

[83] C. A. Vincent, "*Polymer electrolytes*", Prog Solid State Chem, vol. 17, 1987, 145-261.

[84] M. Watanabe, *et al.*, "*Effects of polymer structure and incorporated salt species on ionic conductivity of polymer complexes formed by aliphatic polyester and alkali metal thiocyanate*", Macromolecules, vol. 19, 1986, 188-192.

[85] Gray F M, "*Polymer Electrolytes*", RSC Materials Monographs, The Royal Society of Chemistry, London, 1997.

[86] Mark E. Orazem and Bernard Tribollet, "*Electrochemical impedance spectroscopy*", John Wiley & Sons, 2008.

[87] Maria Plancha, "*Electrólitos poliméricos para sistemas electroquímicos de energia*", Phd Thesis, Technical University of Lisbon, 2008.

[88] Michael E. Brown, "*Introduction to termal analysis: techniques and applications*", Kluwer Academic, 2001.

[89] K. Sreenivas, *et al.*, "*Investigation of Pt/Ti bilayer metallization on silicon for ferroelectric thin film integration*", Journal of Applied Physics, vol. 75, 1994, 232-239.

[90] C. Y. Ting and M. Wittmer, "*The use of titanium-based contact barrier layers in silicon technology*", Thin Solid Films, vol. 96, 1982, 327-345.

[91] S. L. Firebaugh, *et al.*, "*Investigation of high-temperature degradation of platinum thin films with an in situ resistance measurement apparatus*", Journal of Microelectromechamical Systems, vol. 7, n.º 1, 1998, 128-135.

[92] Moon-Soo Park, "*Performance evaluation of printed* $LiCoO_2$ *cathodes with PVDF-HFP gel electrolyte for lithium ion microbatteries*", Electrochimica Acta, vol. 53, 2008, 5523-5527.

[93] L. Predoana, "*Electrochemical properties of the* $LiCoO_2$ *powder obtained by sol-gel method*", Journal of the European Ceramic Society, vol. 27, 2007, 1137-1142.

[94] L. Predoana, *et al.*, "*Advanced techniques for* $LiCoO_2$ *preparation and testing*", Proc. of the International Workshop, Sofia, Bulgaria, 4-9 September de 2004.

[95] H. Y. Park, *et al.*, "*Bias sputtering and characterization of* $LiCoO_2$ *thin film cathodes for thin film microbattery*", Materials Chemistry and Physics, vol. 93, 2005, 70-78.

[96] Powder Diffraction File, Joint Committee on Powder Diffraction Standards, ASTM, Philadelphia, PA, 1967.

[97] J. B. Bates, *et al.*, “*Thin-film lithium and lithium-ion batteries*”, Solid State Ionics, vol. 135, 2000, 33-45.

[98] Y. Hamon, *et al.*, “*Influence of sputtering conditions on ionic conductivity of LIPON thin films*”, Solid State Ionics, vol. 177, 2006, 257-261.

[99] N. J. Dudney and B. J. Neudecker, “*Solid state thin-film lithium battery systems*”, Solid State and Materials Science, vol. 5, 1999, 479-482.

[100] N. J. Dudney, “*Solid-state thin-film rechargeable batteries*”, Materials Science and Engineering B, vol. 116, 2005, 245-249.

[101] Ho Young Park, *et al.*, “*Effects of sputtering pressure on the characteristics of lithium ion conductive lithium phosphorous oxynitride thin film*”, J. Electroceram, vol. 17, 2006, 1023-1030.